LETTER

doi:10.1038/nature10379

In vitro centromere and kinetochore assembly on defined chromatin templates

Annika Guse[1], Christopher W. Carroll[1], Ben Moree[1], Colin J. Fuller[1] & Aaron F. Straight[1]

During cell division, chromosomes are segregated to nascent daughter cells by attaching to the microtubules of the mitotic spindle through the kinetochore. Kinetochores are assembled on a specialized chromatin domain called the centromere, which is characterized by the replacement of nucleosomal histone H3 with the histone H3 variant centromere protein A (CENP-A). CENP-A is essential for centromere and kinetochore formation in all eukaryotes but it is unknown how CENP-A chromatin directs centromere and kinetochore assembly[1]. Here we generate synthetic CENP-A chromatin that recapitulates essential steps of centromere and kinetochore assembly *in vitro*. We show that reconstituted CENP-A chromatin when added to cell-free extracts is sufficient for the assembly of centromere and kinetochore proteins, microtubule binding and stabilization, and mitotic checkpoint function. Using chromatin assembled from histone H3/CENP-A chimaeras, we demonstrate that the conserved carboxy terminus of CENP-A is necessary and sufficient for centromere and kinetochore protein recruitment and function but that the CENP-A targeting domain—required for new CENP-A histone assembly[2]—is not. These data show that two of the primary requirements for accurate chromosome segregation, the assembly of the kinetochore and the propagation of CENP-A chromatin, are specified by different elements in the CENP-A histone. Our unique cell-free system enables complete control and manipulation of the chromatin substrate and thus presents a powerful tool to study centromere and kinetochore assembly.

Metazoan centromeres are specified epigenetically by the presence of CENP-A nucleosomes[3]. Structural differences between CENP-A and histone H3 nucleosomes[2,4] and/or specific protein recognition elements in CENP-A seem to provide the information that specifies centromere identity and directs kinetochore assembly in a DNA-sequence-independent manner[5–10]. Moreover, many metazoan centromeres are complex in their organization, with interspersed blocks of CENP-A nucleosomes and histone H3 nucleosomes assembled on long arrays of repetitive DNA[11–13]. The difficulty in purifying and manipulating complex centromeres has limited our understanding of how centromeric chromatin promotes centromere and kinetochore formation and chromosome segregation.

To mimic the arrays of CENP-A nucleosomes present in complex vertebrate centromeres, we reconstituted human CENP-A chromatin from recombinant components (Fig. 1a). We generated saturated chromatin arrays by salt dialysis of purified histone proteins H2A, H2B, H4 and either CENP-A or H3 with a biotinylated DNA template containing 19 repeats of a 147 bp high-affinity nucleosome positioning sequence (19X601) (Supplementary Fig. 1a, b)[14,15]. We bound the biotinylated arrays to streptavidin-coated magnetic beads, thereby immobilizing the arrays so that they can be easily added to and recovered from cell extracts (Fig. 1a and Supplementary Fig. 1c–e).

We recently demonstrated that the essential centromere protein CENP-C directly recognizes the C terminus of CENP-A in mononucleosomes but not in isolated CENP-A_2/$H4_2$ tetramers[5] (our unpublished observations). Therefore, we tested *in vitro* translated human and *Xenopus laevis* CENP-C for binding to reconstituted H3 and CENP-A chromatin. Human and *Xenopus* CENP-A are >50% identical (Supplementary Fig. 2a) and we find that both human and *Xenopus* CENP-C bind specifically to human CENP-A chromatin arrays *in vitro*, when compared to H3 chromatin arrays (Supplementary Fig. 2b).

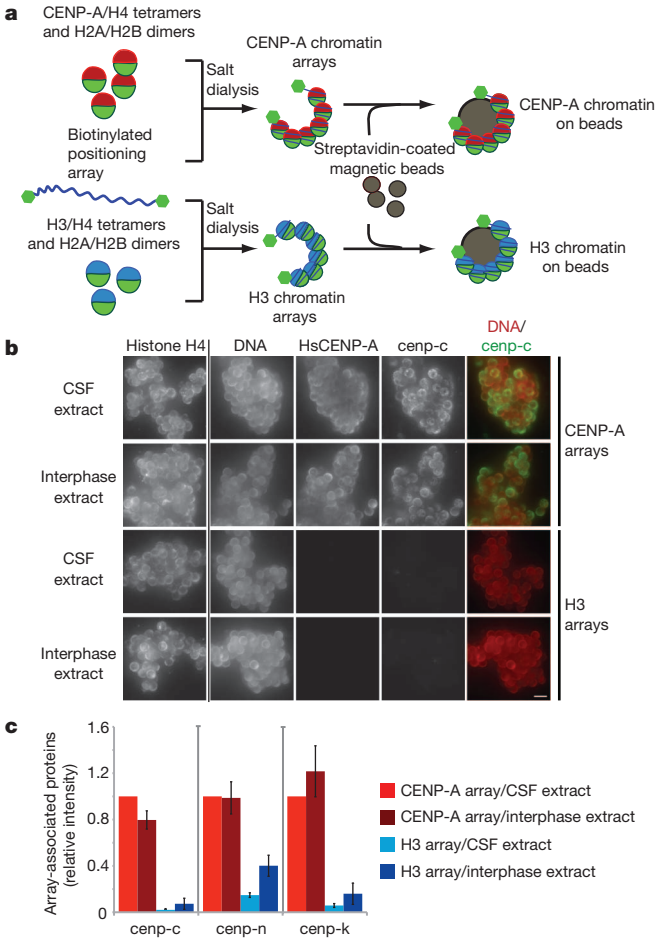

Figure 1 | Reconstituted CENP-A chromatin supports centromere assembly in *Xenopus* egg extracts. **a**, A schematic showing the reconstitution of CENP-A and H3 chromatin arrays and the attachment of the chromatin to magnetic beads via biotin end-labelled DNA. **b**, Representative images comparing cenp-c binding to human CENP-A (HsCENP-A) and H3 chromatin arrays in CSF and interphase *Xenopus* extract. The left column shows the separate histone H4 staining used for normalization of the quantification, followed by staining for DNA, human CENP-A and cenp-c. A merge image of the DNA (red) and cenp-c (green) channels is shown in the right column. Scale bar, 5 μm. **c**, Quantification of the array-associated centromeric proteins cenp-c, cenp-n and cenp-k in CSF and interphase extracts, normalized to histone H4 levels. The levels are rescaled so that CENP-A arrays in CSF are set at 1. Error bars represent the standard error of the mean (s.e.m.), $n = 3$ ($P < 0.05$ between CENP-A and H3 chromatin arrays for cenp-c, cenp-n and cenp-k).

[1]Department of Biochemistry, Stanford Medical School, Beckman 409A, Stanford, California 94305-5307, USA.

Xenopus egg extract is a widely used cell-free system to study chromosome segregation[16]. Egg extracts are arrested in metaphase II of meiosis by the activity of cytostatic factor (CSF) and the cell-cycle state of the extract can be transitioned into interphase by adding calcium. We developed a quantitative immunofluorescence assay to determine whether centromere proteins bound to CENP-A chromatin arrays when arrays were added to *Xenopus* egg extracts. CENP-N and CENP-K are centromere proteins that are required for proper centromere and kinetochore assembly in somatic cells, and we have previously shown that CENP-N, similar to CENP-C, directly binds to the CENP-A nucleosome[6]. We found that cenp-c, cenp-n and cenp-k specifically associated with CENP-A arrays independent of the cell-cycle stage of the extract (Fig. 1b, c and Supplementary Fig. 2c–f). The centromere protein cenp-t that binds to either H3 nucleosomes or DNA at centromeres did not selectively bind CENP-A chromatin arrays (Supplementary Fig. 3a, b)[17]. Similarly, the inner centromere protein incenp and polo-like kinase 1 (plk1) associated with both types of chromatin arrays (Supplementary Fig. 3c). *Xenopus* incenp is targeted to chromatin through phosphorylation of both H2A and H3 and thus may have affinity for both CENP-A and H3 chromatin[18–20] and plk1 associates with chromatin in *Xenopus* egg extract independent of the kinetochore[21]. Furthermore, reconstituted chromatin segments are unlikely to generate paired sister chromatids with inner centromeres because naked DNA and linear DNA replicates inefficiently in these egg extracts[22]. The specific recruitment of the centromere proteins cenp-c, cenp-n and cenp-k, however, indicates that reconstituted CENP-A chromatin arrays can support essential steps in the centromere assembly process *in vitro*.

Functional kinetochores assemble on sperm chromatin in metaphase *Xenopus* egg extract. At high sperm concentration, microtubule depolymerization causes mitotic checkpoint activation, resulting in the increased association of checkpoint proteins with kinetochores and cell-cycle arrest[23]. We tested whether reconstituted CENP-A chromatin arrays support kinetochore assembly and checkpoint protein binding after microtubule depolymerization. We added CENP-A or H3 arrays to CSF-arrested egg extracts and then cycled the extracts through interphase and back into mitosis, in the presence or absence of nocodazole, as outlined in Fig. 2a and demonstrated in Supplementary Fig. 4a. The constitutive centromere protein cenp-c and the microtubule-binding kinetochore protein ndc80 bound to CENP-A arrays in the presence or absence of nocodazole (Fig. 2b, c and Supplementary Fig. 4b). The spindle assembly checkpoint proteins cenp-e, mad2, rod (also known as kntc1) and zw10 associated with CENP-A chromatin at intermediate levels in the absence of nocodazole but upon microtubule depolymerization their binding increased 2–4 fold (Fig. 2b). Western blot analysis showed that cenp-c and ndc80 are precipitated with CENP-A arrays independent of microtubule depolymerization. *Xenopus* zw10 and rod are enriched on CENP-A arrays upon nocodazole treatment in metaphase, regardless of whether the extract has been cycled through interphase (Fig. 2c). These results indicate that CENP-A chromatin arrays respond to microtubule depolymerization by recruiting mitotic checkpoint proteins (Fig. 2b, c and Supplementary Fig. 4b).

Microtubule binding is a hallmark of kinetochore function and decondensed sperm chromatin efficiently supports spindle formation in egg extracts (Fig. 3a, left)[24]. However, chromatin assembled on naked DNA induces spindle formation in *Xenopus* egg extracts independent of kinetochores[25]. When we added CENP-A and H3 chromatin beads into mitotic egg extract we observed microtubule polymerization around the majority of CENP-A arrays but only around a subset of H3 arrays (Fig. 3a, left). We quantified the amount of microtubule polymer associated with each type of array and found significantly more microtubules associated with CENP-A chromatin beads (Fig. 3b and Supplementary Fig. 5a). This indicates that CENP-A chromatin preferentially stabilizes microtubules or promotes their polymerization. We observed heterogeneous microtubule structures around the CENP-A chromatin beads ranging from bipolar spindles to stabilized

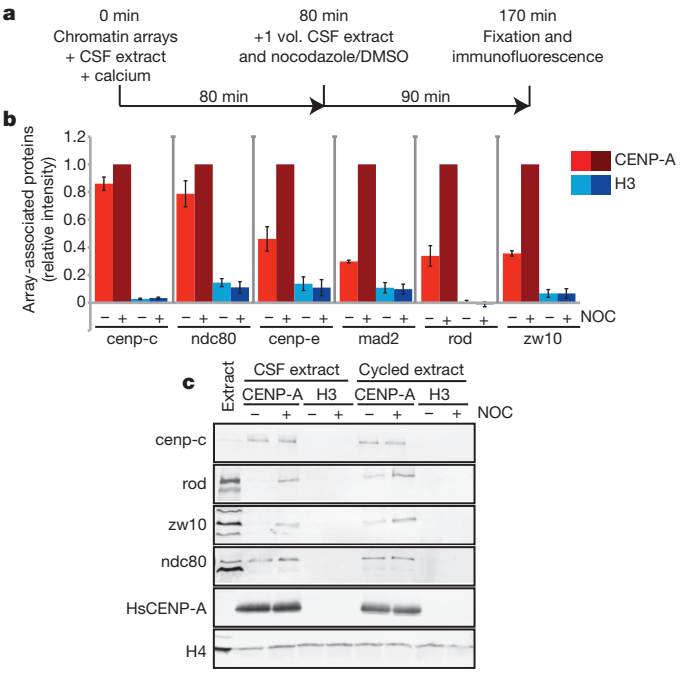

Figure 2 | CENP-A chromatin specifically recruits kinetochore proteins as a response to a mimic of kinetochore detachment from microtubules. **a**, A schematic showing the experimental procedure. **b**, Quantification of immunofluorescence analysis of cenp-c, ndc80, cenp-e, mad2, rod or zw10 recruitment to chromatin arrays with (+) and without (−) nocodazole (NOC). The levels are rescaled so that CENP-A arrays with nocodazole are set at 1. Error bars represent s.e.m., $n = 3$ ($P < 0.05$ between (−) and (+) nocodazole for cenp-e, mad2, rod and zw10 binding to CENP-A chromatin arrays). **c**, Western blot analysis of cenp-c, ndc80, rod and zw10 recruitment to CENP-A (HsCENP-A) and H3 chromatin arrays with and without nocodazole in CSF and cycled egg extracts. H4 levels are shown as a loading control.

microtubules or microtubule bundles (Fig. 3a and Supplementary Fig. 5a, b). A second property of functional kinetochores is that kinetochore-associated microtubule bundles (k-fibres) are stable to cold treatment, which depolymerizes non-kinetochore microtubules. We asked whether kinetochores assembled on CENP-A chromatin could stabilize microtubules to cold shock by incubating the microtubule assembly reactions for 10 min at 4 °C. We found that kinetochores assembled on CENP-A chromatin arrays stabilized microtubules to cold shock similar to kinetochores assembled on native sperm chromatin whereas H3 chromatin arrays did not (Fig. 3a, c and Supplementary Fig. 5c). When we completely depolymerized microtubules with nocodazole we observed mad2 recruitment to native sperm centromeres and CENP-A chromatin beads but not H3 chromatin beads (Fig. 3a, c and Supplementary Fig. 5c). These results indicate that CENP-A chromatin arrays, similar to native sperm chromatin, assemble functional kinetochores that promote microtubule binding, k-fibre stabilization and spindle checkpoint function (Fig. 3a).

In cells, unattached kinetochores activate the mitotic checkpoint and delay mitotic exit until all chromosomes are properly attached and aligned[26,27]. We tested whether kinetochores assembled on CENP-A chromatin arrays could generate a mitotic checkpoint response to microtubule depolymerization and delay the cell cycle. We mixed CENP-A and H3 chromatin with CSF extracts, cycled the reactions through interphase and then cycled them back into mitosis in the presence or absence of nocodazole (Fig. 2a). We then released the extract from mitosis into interphase a second time and monitored the kinetics of this transition by measuring the mitosis-specific phosphorylation of wee1 (phospho-wee1) (Fig. 3d). On release from mitosis, phospho-wee1 levels rapidly declined and were undetectable after 30 min in control extracts containing CENP-A chromatin or H3 chromatin, as well as in extracts containing H3 chromatin in the presence of

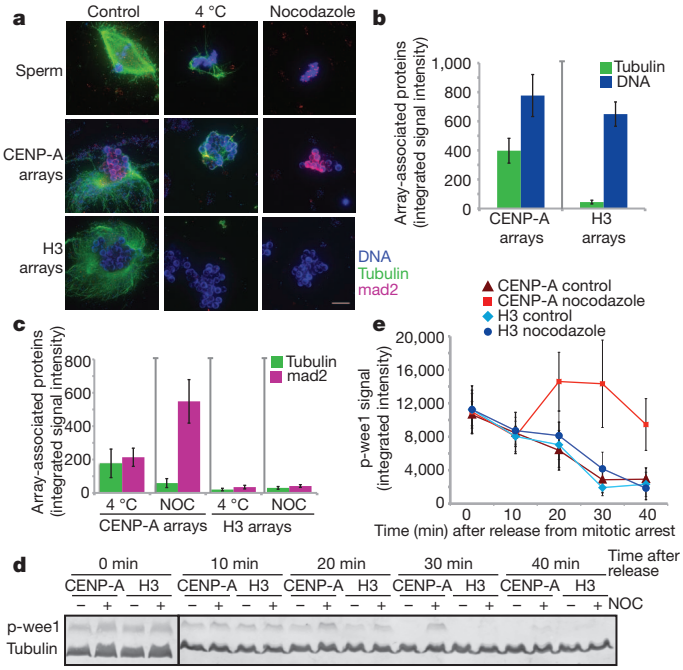

Figure 3 | Kinetochores assembled on reconstituted CENP-A chromatin bind microtubules and generate a mitotic checkpoint signal.
a, Representative images of microtubule polymerization induced by sperm or reconstituted CENP-A and H3 chromatin. Microtubules (green) and mad2 (magenta) levels are shown. Scale bar, 10 μm. **b**, Quantification of tubulin and DNA associated with CENP-A and H3 chromatin beads. Error bars represent s.e.m., $n = 5$. **c**, Quantification of tubulin and mad2 levels associated with CENP-A and H3 chromatin beads after cold shock (4 °C) and nocodazole (NOC) treatment. Error bars represent s.e.m., $n = 5$. **d**, Western blot showing phospho-wee1 (p-wee1) levels as an indicator of the cell-cycle stage and tubulin levels as a loading control. Samples from different time points after release from mitotic arrest are shown for CENP-A and H3 chromatin arrays, each incubated with nocodazole (+) or with DMSO (−) as a control. **e**, Quantification of four independent experiments showing the phospho-wee1 signal intensity (p-wee1 signal) over time (min). Error bars represent s.e.m., $n = 4$.

nocodazole (Fig. 3d, e). In extracts containing CENP-A chromatin and nocodazole, the phospho-wee1 signal increased until 20 min after calcium addition and subsequently declined until 40 min after calcium addition to a level only slightly lower than that before release (Fig. 3d, e). In the presence of CENP-A chromatin and nocodazole, cyclin B levels rapidly declined but then stabilized, similar to the response observed for native sperm chromatin[23]. However, cyclin B was not stabilized in the presence of H3 chromatin and nocodazole (Supplementary Fig. 5d, e). We estimate that the number of CENP-A nucleosomes we are adding to the egg extract exceeds the CENP-A nucleosome concentration required to activate the checkpoint using sperm nuclei[23]. The lower efficiency of reconstituted arrays for checkpoint signalling may be due to the comparatively short length of our reconstituted CENP-A chromatin to native CENP-A chromatin or the lack of replicated sister chromatids and inner centromeres important for tension-dependent checkpoint activation. Despite these differences, our synthetic CENP-A chromatin supports a mitotic checkpoint response that mimics the response of native kinetochores to microtubule depolymerization.

The reconstituted chromatin system we have developed provides a distinct experimental advantage over native metazoan centromeric chromatin because the chromatin template can be easily manipulated to dissect the roles of histone proteins in centromere function. A central question in centromere function is how CENP-A chromatin directs the assembly of the centromere and kinetochore. CENP-N recognizes the CATD region of the CENP-A nucleosome while CENP-C binds the C-terminal tail of CENP-A[5,6]. However, the relative importance of these two recognition mechanisms in centromere and kinetochore assembly is incompletely understood.

We generated chromatin arrays containing chimaeric CENP-A/H3 proteins to ask how the CENP-A CATD domain and the CENP-A C terminus influence centromere and kinetochore assembly (Fig. 4a). We characterized the level of histone exchange and/or loss from the arrays during incubation in extracts and found that the majority of recombinant human CENP-A nucleosomes were stable during the incubation, indicating low exchange and/or loss rates (Supplementary Fig. 6a, b). We detected a low level of phosphorylated histone H3 on CENP-A chromatin arrays in CSF extract (11.7% ± 7% compared to H3 arrays) and in extract that had been cycled through interphase and back into mitosis (22% ± 13% compared to H3 arrays) (Supplementary Fig. 6c, d). The chimaeric arrays containing CENP-A with the histone H3 tail (CENP-A + H3C) exhibited similar levels of exchange (Supplementary Fig. 6c, d). The *Xenopus* cenp-a present in the extract did not appreciably exchange onto any of the arrays (detection limit ~5–10% exchange) (Supplementary Fig. 6c). The absence of gross rearrangements or bulk histone exchange suggests that chromatin arrays can be used to dissect how individual domains of CENP-A influence kinetochore assembly.

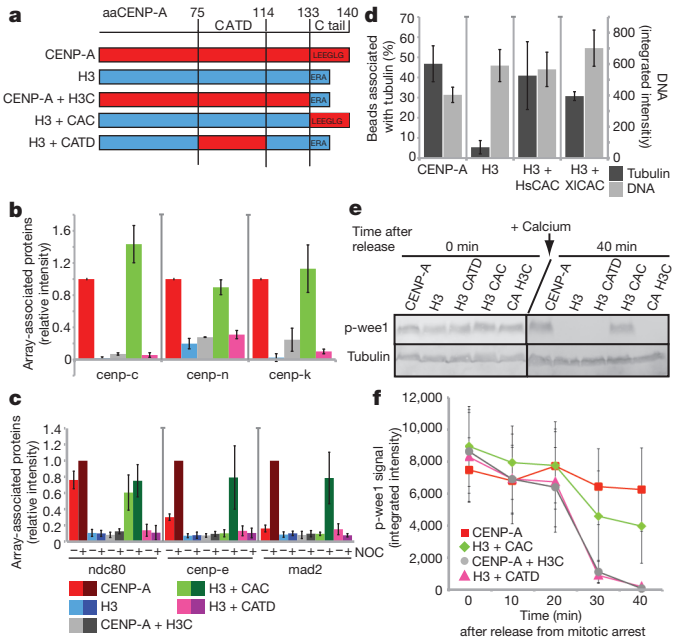

Figure 4 | The CENP-A C terminus is required for centromere and kinetochore assembly in *Xenopus* egg extract. **a**, A schematic showing the different CENP-A/H3 chimaeras used in this study. The numbers at the top represent the amino acid (aa) within human CENP-A. **b**, Quantification of immunofluorescence analysis of cenp-c, cenp-k and cenp-n recruitment to wild-type and chimaeric arrays. The relative amounts of each centromere protein bound to the arrays are shown relative to CENP-A arrays set to 1. Error bars represent s.e.m., $n = 3$ ($P \leq 0.05$ for all proteins binding to CENP-A arrays compared to chimaeric arrays except for the H3 arrays containing the CENP-A C terminus). **c**, Quantification of immunofluorescence analysis of ndc80, cenp-e, mad2 recruitment to chimaeric chromatin arrays with (+) and without (−) nocodazole (NOC). Values are displayed relative to CENP-A arrays in the presence of nocodazole set to 1. Error bars represent s.e.m., $n = 4$. The efficiencies of recruitment of kinetochore proteins to CENP-A and H3 + CAC arrays in nocodazole were not statistically distinguishable ($P \geq 0.26$ for ndc80, cenp-e and mad2). **d**, Quantification of microtubule binding to CENP-A, H3, H3 + human CAC (HsCAC) and H3 + *Xenopus* CAC (XlCAC) chromatin arrays represented as percentage of beads associated with tubulin levels above threshold (dark grey bars, left *y*-axis). Average DNA levels on chromatin beads are shown representing the levels of chromatin arrays bound to beads (light grey bars, right *y*-axis). Error bars represent s.e.m., $n = 4$ for CENP-A and H3 arrays, $n = 5$ for H3 + human CAC arrays and $n = 2$ for H3 + *Xenopus* CAC arrays. **e**, Western blot analysis shows phospho-wee1 (p-wee1) levels as an indicator of the cell-cycle stage at 0 min and 40 min after mitotic exit. Tubulin levels are shown as a loading control. **f**, Quantification of the phospho-wee1 signal intensity over time. Error bars represent s.e.m., $n = 5$.

Using our *in vitro* centromere and kinetochore assembly assay, we found that cenp-c bound with equal efficiency to chromatin arrays assembled with either wild-type CENP-A or with chimaeras of histone H3 with the CENP-A C-terminal six amino acids (H3 + CAC) but not CENP-A + H3C (Fig. 4b and Supplementary Fig. 7a, left). This demonstrates that the CENP-A C terminus is necessary and sufficient for recruiting cenp-c to CENP-A chromatin arrays in egg extracts, as it is for CENP-A mononucleosome binding *in vitro*[5].

Xenopus cenp-k depends on cenp-c for its association with sperm centromeres[28] and cenp-k also associated with the wild-type and H3 + CAC arrays (Fig. 4b and Supplementary Fig. 7a). Surprisingly, we found that H3 + CAC arrays recruited cenp-n as efficiently as wild-type CENP-A arrays, even though these arrays lack the CATD recognition element for CENP-N[6]. *Xenopus* cenp-n binding to either CENP-A + H3C or H3 + CATD arrays was no better than its binding to H3 chromatin arrays, indicating that the CENP-A C terminus is required for cenp-n association with CENP-A chromatin in *Xenopus* egg extract (Fig. 4b and Supplementary Fig. 7a). The lack of *Xenopus* cenp-n binding to H3 + CATD and CENP-A + H3C chromatin arrays is not due to species differences because *Xenopus* cenp-n binds human CENP-A mononucleosomes *in vitro* in the absence of CENP-C (Supplementary Fig. 7b). The association of cenp-n and cenp-k with chromatin arrays was dependent on cenp-c, as cenp-c depletion from the extract (Supplementary Fig. 8a) reduced the binding to background levels (Supplementary Fig. 8b, c). This was not due to depletion of cenp-n or cenp-k by cenp-c, as we have previously shown that complementation of cenp-c-depleted extracts restores cenp-k binding and CENP-K is known to depend on CENP-N for its centromere localization[6,28,29,30]. The dependence of CENP-N on CENP-C for its localization to CENP-A arrays may reflect a role for CENP-C in altering the geometry of centromeric chromatin to promote access of CENP-N to CENP-A nucleosomes, or it may reflect the assembly of CENP-N into the larger CCAN complex recruited to the centromere via CENP-C. Our results demonstrate that cenp-c recognition of the CENP-A C terminus is necessary and sufficient for cenp-n and cenp-k association with chromatin arrays in *Xenopus* egg extract.

We analysed the chromatin requirements for mitotic kinetochore formation using the experimental strategy illustrated in Fig. 2a. The kinetochore proteins ndc80, cenp-e, mad2, rod and zw10 are efficiently recruited to wild-type and H3 + CAC chromatin arrays, but not to CENP-A + H3C or H3 + CATD chromatin arrays (Fig. 4c, Supplementary Fig. 9a and Supplementary Fig. 10a). Similar to wild-type CENP-A chromatin, only the checkpoint proteins cenp-e, mad2, zw10 and rod increased in their association with H3 + CAC after microtubule depolymerization (Fig. 4c, Supplementary Fig. 9a and Supplementary Fig. 10a). As with wild-type CENP-A arrays, the H3 + CAC arrays showed increased associated microtubule polymer indicating that the C terminus of CENP-A directs the formation of microtubule binding or stabilization activity (Fig. 4d). Human and *Xenopus* CENP-A differ by two amino acids in their C-terminal tail (Supplementary Fig. 2a) and chimaeric nucleosome arrays containing the *Xenopus* C-terminal tail of cenp-a fused to H3 (H3 + *Xenopus* CAC) were equally efficient in cenp-c recruitment and microtubule binding as human H3 + CAC arrays (Fig. 4d and Supplementary Fig. 10b); indicating that the mode of interaction between CENP-C and CENP-A is conserved.

We assayed the ability of chimaeric nucleosome arrays to promote mitotic checkpoint arrest after microtubule depolymerization and found that H3 + CATD and CENP-A + H3C did not delay the exit from mitosis but that H3 + CAC did (Fig. 4e, f). The delay of mitotic exit caused by H3 + CAC arrays was less effective than that of CENP-A chromatin arrays, indicating that regions of CENP-A in addition to the C terminus increase the effectiveness of checkpoint signalling, possibly by stabilizing CCAN and kinetochore protein interactions with chromatin (Fig. 4e, f). Taken together, our data demonstrate that the primary chromatin determinant for functional centromere and kinetochore assembly is the C terminus of CENP-A and its recognition by CENP-C.

Here we have shown that reconstituted CENP-A chromatin, in the absence of native centromeric DNA, is necessary and sufficient for centromere and kinetochore assembly. Our data imply that short domains of CENP-A chromatin are sufficient for assembling core components of the centromere and kinetochore in the absence of higher-order organization of centromeric chromatin and interspersed domains of H3 chromatin.

Using our *in vitro* system, we have directly assessed how domains of CENP-A participate in centromere and kinetochore assembly, even when the mutations we analyse would be expected to be lethal *in vivo*. We find that the CENP-A C terminus is both necessary and sufficient for the recruitment of centromere and kinetochore proteins, for microtubule binding and for a checkpoint response to microtubule depolymerization. We suggest that CENP-A performs two functions that can be separated molecularly: (1) the CENP-A CATD provides a recognition mechanism for targeting of CENP-A to centromeres to maintain centromeric chromatin[2,6–8]; and (2) the CENP-A C-terminal tail domain recruits the conserved centromere protein CENP-C to promote centromere and kinetochore assembly[5]. We envision the use of more complex chromatin templates to understand the importance of higher-order chromatin organization and regulatory modifications in centromere assembly and function.

METHODS SUMMARY

Histone proteins and chimaeras were purified as described previously[5,6,15] and assembled onto a biotin end-labelled tandem array of 19 high-affinity nucleosome positioning sequences (19X601) by salt dialysis[14]. Chromatin arrays were bound to streptavidin-coated magnetic Dynabeads (Invitrogen). *X. laevis* extracts were prepared as previously described[16] and centromere protein binding to chromatin arrays was performed in freshly prepared CSF egg extract for 1 h with or without calcium addition. Arrays were fixed in formaldehyde and stained for centromere proteins by indirect immunofluorescence. Kinetochore and checkpoint protein assembly was assayed by adding arrays to extracts released into interphase with calcium for 80 min followed by re-addition of CSF extract in the presence or absence of nocodazole (10 $\mu g\,ml^{-1}$) for another 90 min. To analyse microtubule binding, chromatin arrays were incubated in CSF for 90 min. Reactions were sedimented through a glycerol cushion onto a coverslip followed by tubulin immunofluorescence. Chromatin-array-dependent inhibition of mitotic exit was assayed as described for kinetochore protein binding, but calcium was added a second time to release extracts into interphase. The cell-cycle state was monitored by western blotting using anti-phospho-wee1 antibody, provided by J. E. Ferrell.

Images were collected as 13 axial planes at 2 μm intervals on a Nikon Eclipse-80i microscope using a ×60, 1.4 NA PlanApo oil lens and a CoolSnapHQ CCD camera (Photometrics) with MetaMorph software (MDS Analytical Technologies). Axial stacks were maximum intensity projected and quantified using custom software. For normalization of each experiment, a separate histone H4 staining was performed to quantify the exact array coupling efficiency.

Full Methods and any associated references are available in the online version of the paper at www.nature.com/nature.

Received 18 November 2010; accepted 19 July 2011.
Published online 28 August 2011.

1. Cheeseman, I. M. & Desai, A. Molecular architecture of the kinetochore-microtubule interface. *Nature Rev. Mol. Cell Biol.* **9,** 33–46 (2008).
2. Black, B. E. *et al.* Structural determinants for generating centromeric chromatin. *Nature* **430,** 578–582 (2004).
3. Black, B. E. & Bassett, E. A. The histone variant CENP-A and centromere specification. *Curr. Opin. Cell Biol.* **20,** 91–100 (2008).
4. Sekulic, N., Bassett, E. A., Rogers, D. J. & Black, B. E. The structure of $(CENP\text{-}A\text{-}H4)_2$ reveals physical features that mark centromeres. *Nature* **467,** 347–351 (2010).
5. Carroll, C. W., Milks, K. J. & Straight, A. F. Dual recognition of CENP-A nucleosomes is required for centromere assembly. *J. Cell Biol.* **189,** 1143–1155 (2010).
6. Carroll, C. W., Silva, M. C. C., Godek, K. M., Jansen, L. E. T. & Straight, A. F. Centromere assembly requires the direct recognition of CENP-A nucleosomes by CENP-N. *Nature Cell Biol.* **11,** 896–902 (2009).
7. Dunleavy, E. M. *et al.* HJURP is a cell-cycle-dependent maintenance and deposition factor of CENP-A at centromeres. *Cell* **137,** 485–497 (2009).
8. Foltz, D. R. *et al.* Centromere-specific assembly of CENP-A nucleosomes is mediated by HJURP. *Cell* **137,** 472–484 (2009).

9. Hu, H. *et al.* Structure of a CENP-A-histone H4 heterodimer in complex with chaperone HJURP. *Genes Dev.* **25,** 901–906 (2011).
10. Tachiwana, H. *et al.* Crystal structure of the human centromeric nucleosome containing CENP-A. *Nature.* doi:10.1038/nature10258 (10 July, 2011).
11. Blower, M. D., Sullivan, B. A. & Karpen, G. H. Conserved organization of centromeric chromatin in flies and humans. *Dev. Cell* **2,** 319–330 (2002).
12. Ribeiro, S. *et al.* A super-resolution map of the vertebrate kinetochore. *Proc. Natl Acad. Sci. USA* **107,** 10484–10489 (2010).
13. Zinkowski, R. P., Meyne, J. & Brinkley, B. R. The centromere-kinetochore complex: a repeat subunit model. *J. Cell Biol.* **113,** 1091–1110 (1991).
14. Huynh, V., Robinson, P. & Rhodes, D. A method for the *in vitro* reconstitution of a defined "30 nm" chromatin fibre containing stoichiometric amounts of the linker histone. *J. Mol. Biol.* **345,** 957–968 (2005).
15. Luger, K., Rechsteiner, T. J., Flaus, A. J., Waye, M. M. & Richmond, T. J. Characterization of nucleosome core particles containing histone proteins made in bacteria. *J. Mol. Biol.* **272,** 301–311 (1997).
16. Desai, A., Murray, A., Mitchison, T. J. & Walczak, C. E. The use of *Xenopus* egg extracts to study mitotic spindle assembly and function *in vitro*. *Methods Cell Biol.* **61,** 385–412 (1999).
17. Hori, T. *et al.* CCAN makes multiple contacts with centromeric DNA to provide distinct pathways to the outer kinetochore. *Cell* **135,** 1039–1052 (2008).
18. Kawashima, S. A., Yamagishi, Y., Honda, T., Ishiguro, K.-i. & Watanabe, Y. Phosphorylation of H2A by Bub1 prevents chromosomal instability through localizing shugoshin. *Science* **327,** 172–177 (2010).
19. Kelly, A. E. *et al.* Survivin reads phosphorylated histone H3 threonine 3 to activate the mitotic kinase Aurora B. *Science* **330,** 235–239 (2010).
20. Wang, F. *et al.* Histone H3 Thr-3 phosphorylation by Haspin positions Aurora B at centromeres in mitosis. *Science* **330,** 231–235 (2010).
21. Budde, P. P., Kumagai, A., Dunphy, W. G. & Heald, R. Regulation of Op18 during spindle assembly in *Xenopus* egg extracts. *J. Cell Biol.* **153,** 149–158 (2001).
22. Blow, J. J. & Laskey, R. A. Initiation of DNA replication in nuclei and purified DNA by a cell-free extract of *Xenopus* eggs. *Cell* **47,** 577–587 (1986).
23. Minshull, J., Sun, H., Tonks, N. K. & Murray, A. W. A MAP kinase-dependent spindle assembly checkpoint in *Xenopus* egg extracts. *Cell* **79,** 475–486 (1994).
24. Sawin, K. E. & Mitchison, T. J. Mitotic spindle assembly by two different pathways *in vitro*. *J. Cell Biol.* **112,** 925–940 (1991).
25. Heald, R. *et al.* Self-organization of microtubules into bipolar spindles around artificial chromosomes in *Xenopus* egg extracts. *Nature* **382,** 420–425 (1996).
26. Nicklas, R. B., Ward, S. C. & Gorbsky, G. J. Kinetochore chemistry is sensitive to tension and may link mitotic forces to a cell cycle checkpoint. *J. Cell Biol.* **130,** 929–939 (1995).
27. Rieder, C. L., Cole, R. W., Khodjakov, A. & Sluder, G. The checkpoint delaying anaphase in response to chromosome monoorientation is mediated by an inhibitory signal produced by unattached kinetochores. *J. Cell Biol.* **130,** 941–948 (1995).
28. Milks, K. J., Moree, B. & Straight, A. F. Dissection of CENP-C-directed centromere and kinetochore assembly. *Mol. Biol. Cell* **20,** 4246–4255 (2009).
29. Foltz, D. R. *et al.* The human CENP-A centromeric nucleosome-associated complex. *Nature Cell Biol.* **8,** 458–469 (2006).
30. McClelland, S. E. *et al.* The CENP-A NAC/CAD kinetochore complex controls chromosome congression and spindle bipolarity. *EMBO J.* **26,** 5033–5047 (2007).

Supplementary Information is linked to the online version of the paper at www.nature.com/nature.

Acknowledgements The authors would like to thank A.F.S. laboratory members for support and comments, J. E. Ferrell, A. Murray, R.-H. Chen, G. Kops and P. T. Stukenberg for providing antibodies. D. Rhodes, P. Robinson, K. Luger, J. Hansen, G. Narlikar and J. Yang for providing reagents and advice. A.G. was supported by a postdoctoral fellowship from the German Research Foundation (DFG). C.W.C. was supported by a postdoctoral fellowship from the Helen Hay Whitney Foundation and the American Heart Association (AHA). B.M. was supported by T32GM007276, C.J.F. was supported by a Stanford Graduate Fellowship and this work was supported by National Institutes of Health (NIH) R01GM074728 to A.F.S.

Author Contributions A.G. and A.F.S. designed the experiments and wrote the manuscript. A.G. performed all the experiments. C.W.C. purified the CENP-A/H3 chimaeras and assembled arrays containing chimaeric proteins, analysed *Xenopus* cenp-n binding to human CENP-A mononucleosomes and provided advice. B.M. generated *Xenopus* centromere protein antibodies and C.J.F. designed and wrote the image analysis software for quantitative analysis.

Author Information Reprints and permissions information is available at www.nature.com/reprints. The authors declare no competing financial interests. Readers are welcome to comment on the online version of this article at www.nature.com/nature. Correspondence and requests for materials should be addressed to A.F.S. (astraigh@stanford.edu).

METHODS

Histone expression. CENP-A/H4 and H3/H4 wild-type and chimaeric tetramers, as well as H2A and H2B dimers were expressed and purified as described previously[5,6,15,31].

Preparation of biotinylated array DNA. A tandem array of 19 copies of the high-affinity nucleosome positioning sequence (19X601)[14,32] was digested with EcoRI, XbaI, DraI and HaeII (NEB) overnight to excise the 19-nucleosome positioning sequence array and to digest the remaining backbone DNA to smaller DNA fragments. The array DNA was then purified by PEG precipitation and dialysed against 10 mM Tris-HCl pH 8.0, 0.25 mM EDTA as previously described[14].

The array DNA was end labelled with biotin by end filling the EcoRI and XbaI sites using Klenow DNA polymerase for 4 h at 37 °C in a reaction containing 35 μM Biotin-14-dATP (Invitrogen), α-thio-dTTP and α-thio-dGTP (Chemcyte) and dCTP. The labelled DNA was then purified using a PCR fragment purification kit (Qiagen). The biotinylation efficiency was determined by adding FITC-streptavidin (final concentration of 10 μg ml^{-1}) to 500 ng of purified array DNA and monitoring the fraction of gel-shifted DNA after migration in a 0.7% agarose gel.

Chromatin array assembly. To assemble chromatin arrays, biotinylated DNA, CENP-A/H4 or H3/H4 tetramers and H2A/H2B dimers were mixed at a stochiometry of 1:1:2.2 or 1:0.9:2.2, respectively, in high-salt buffer (10 mM Tris-HCl pH 7.5, 0.25 mM EDTA, 2 M NaCl) and then dialysed into low-salt buffer (10 mM Tris-HCl pH 7.5, 0.25 mM EDTA, 2.5 mM NaCl) over 60–70 h at 4 °C. Final array DNA concentration typically was 0.15 mg ml^{-1} to 0.2 mg ml^{-1}.

To assess the efficiency of nucleosome assemblies, arrays were digested at room temperature (approximately 22 °C) overnight with AvaI in a low-magnesium buffer (50 mM potassium acetate, 20 mM Tris-acetate, 0.5 mM magnesium acetate, 1 mM dithiothreitol, pH 7.9). Digested chromatin arrays were supplemented with glycerol (20% final concentration) and separated on a native 5% acrylamide gel in 0.5× Tris/Borate/EDTA buffer for 80 min at 10 mA. Gels were stained with EtBr (1 μg ml^{-1}) to visualize DNA.

Coupling of biotinylated chromatin arrays to Dynabeads. Biotinylated chromatin arrays were coupled to prewashed streptavidin-coated magnetic Dynabeads (Invitrogen) at a ratio of 10 μg DNA to 1 mg beads in 50 mM Tris-HCl pH 8.0, 75 mM NaCl, 0.25 mM EDTA, 2.5% polyvinyl alcohol (PVA) and 0.05% Triton-X-100 for 1–2 h. The beads were then equilibrated in 75 mM Tris-HCl pH 8.0, 75 mM NaCl, 0.25 mM EDTA, 0.05% Triton-X-100 and either used directly or stored at 4 °C for later use.

***X. laevis* egg extracts.** *X. laevis* CSF extracts were prepared as previously described[16,33]. To assess the binding of centromeric proteins to chromatin arrays in CSF and interphase egg extracts, chromatin arrays were mixed with freshly prepared CSF egg extract with or without $CaCl_2$ (final concentration 0.6 mM) at a nucleosome concentration of ~100 nM unless stated otherwise. The reactions were incubated for 1 h at 4 °C or at 16–20 °C in a water bath, the arrays were re-isolated from extracts by exposure to a magnet and then washed three times in 1× CSF-XB buffer (10 mM HEPES pH 7.7, 2 mM $MgCl_2$, 0.1 mM $CaCl_2$, 100 mM KCl, 5 mM EGTA, 50 mM sucrose) supplemented with 0.05% Triton-X-100. Chromatin arrays were fixed in CSF-XB buffer, 0.05% Triton-X-100, 2% formaldehyde for 5 min. After fixation, chromatin arrays were washed into antibody dilution buffer (20 mM Tris-HCl pH 7.5, 150 mM NaCl, 0.1% Triton-X-100, 2% BSA) and analysed by immunofluorescence.

Kinetochore and spindle checkpoint protein assembly were analysed by mixing chromatin arrays with CSF extract and $CaCl_2$ (final concentration 0.6 mM). Reactions were incubated at 16–20 °C for 80 min to allow extracts to release into interphase and mixed every 15 min. One volume of fresh CSF extract was added together with nocodazole (or DMSO) at 10 μg ml^{-1} and samples were held at 16–20 °C for another 90 min. After 170 min total incubation time, samples for immunofluorescence analysis were washed and fixed as described above.

The cell-cycle state was verified by loading 2 μl extract of all relevant time points onto SDS–PAGE, followed by western blotting using the anti-phospho-wee1 antibody[34].

To assess the ability of chromatin arrays to inhibit mitotic exit, arrays were mixed with CSF extract and $CaCl_2$ (final concentration: 0.6 mM). The samples were incubated for 80 min to induce the release into interphase. In the next step, one volume of fresh CSF extract, supplemented with nocodazole/DMSO, was added to cycle the extract back into a mitotic arrest. After 90 min, $CaCl_2$ was added again to release the extract from mitotic arrest. Western blot samples were taken at all indicated time points and processed as described.

To analyse microtubule binding by CENP-A and H3 chromatin arrays, chromatin arrays were mixed with CSF extract and incubated for 90 min at 18–20 °C. During incubation samples were mixed every 15 min. Reactions were fixed for 10 min in 2.5% formaldehyde, sedimented through a glycerol cushion onto coverslips and post-fixed for 5 min in ice-cold methanol followed by immunofluorescence analysis[35]. To assay for mad2 levels and microtubule stabilization, reactions were either supplemented with nocodazole at a final concentration of 10 μg ml^{-1} or shifted to 4 °C for 10 min after the 90 min incubation time.

Immunodepletion. Depletion of *Xenopus* cenp-c from *Xenopus* egg extracts was performed as described previously[28].

Cloning and antibody generation. The *X. laevis* cenp-n cDNA clone (GenBank accession number BC084956) was purchased from American Type Culture Collection. Peptides against *Xenopus* cenp-n (acetyl-CPHKARNSFKITEKR-amide) were synthesized by Bio-Synthesis and peptide antibodies were generated as previously described[36].

Immunofluorescence. For immunofluorescence analysis, fixed chromatin arrays were bound to poly-L-lysine-coated acid-washed coverslips. The following primary antibodies were used for immunofluorescence staining and typically incubated at 4 °C overnight: anti-human CENP-A[30] was directly coupled to Alexa 647 (Molecular Probes), anti-H4 (Abcam), anti-*Xenopus* cenp-c, anti-*Xenopus* cenp-e, anti-*Xenopus* cenp-k and anti-*Xenopus* cenp-n and anti-tubulin (Dm1α; Sigma). Rabbit antibodies were generated against the full-length *Xenopus* polo kinase made in Sf9 cells and a GST fusion to the first 379 amino acids of *Xenopus* incenp made in *E. coli*. The anti-mad2 antibody was provided by A. Murray (Harvard University), and R.-H. Chen (Institute of Molecular Biology, Academia Sinica), the anti-*Xenopus* zw10 and anti-*Xenopus* rod antibodies were provided by G. Kops (University Medical Center Utrecht) and the anti-*Xenopus* ndc80 antibody was provided by P. Todd Stukenberg (University of Virginia). Alexa-conjugated secondary antibodies were used at 1 μg ml^{-1} (Molecular Probes). Propidium iodide at 1 μg ml^{-1} or Hoechst at 10 μg ml^{-1} was used to visualize DNA.

Microscopy and analysis. Images were collected on a Nikon Eclipse 80i microscope using a ×60, 1.4 NA Plan Apo VC oil immersion lens, a Sedat Quad filter set (Chroma Technology) using MetaMorph software (MDS Analytical Technologies) and a charge-coupled device camera (CoolSnapHQ; Photometrics). Thirteen axial planes at 2 μm intervals were acquired with an MFC-2000 Z-axis drive (Applied Scientific Instrumentation). Axial stacks were maximum intensity projected and then quantified using custom software (Matlab) to identify beads in each image and to quantify the integrated intensity for each channel after background subtraction. Briefly, the propidium iodide stained (DNA) channel was used to find beads. Bead centroids were found by filtering the image using a structuring element that had a peak at a 17 pixel radial distance from the structuring element centre, corresponding to the bright ring seen around the edges of the beads. A 35 pixel diameter circle around the centroid of each bead identified was used as the region of interest for that bead. After beads were identified, regions of interest were transferred automatically to the remaining channels and the integrated signal intensity was calculated for each bead in each channel, normalized to the area of the bead region (which was uniform except in cases of partially overlapping beads), and background corrected using an average of three bead-sized regions manually chosen to be away from any beads. For each experiment, at least three images per coverslip were acquired and 20–300 beads were analysed per image. For the normalization of each experiment, a separate histone H4 staining was performed to quantify the exact coupling efficiency for each type of chromatin array and for each experiment.

Immunofluorescence microscopy images of the microtubule binding assays that were subjected to deconvolution were acquired with an Olympus IX70 microscope. The microscope was outfitted with a Deltavision Core system (Applied Precision) using an Olympus ×60 1.4NA Plan Apo lens, a Sedat Quad filter set (Semrock) and a CoolSnap HQ CCD Camera (Photometrics). The microscope was controlled via softworx 4.1.0 software (Applied Precision) and images were deconvolved using softworx v. 4.1.0 (Applied Precision). Microtubule quantification was performed using a modification of the same software used for centromere protein quantification.

Immunoblotting. Western blot samples were separated by SDS–PAGE and transferred onto PVDF membrane (Bio-Rad) in CAPS transfer buffer (10 mM 3-(cyclohexylamino)-1-propanesulfonic acid, pH 11.3, 0.1% SDS and 20% methanol). The following primary antibodies were typically incubated overnight at 4 °C: anti-*Xenopus* cenp-c[28], anti-tubulin (Dm1α, Sigma), anti-H4 (Abcam), anti-phospho H3 (Ser10) (Millipore), anti-phospho-wee1. The anti-phospho-wee1 antibody was provided by J. E. Ferrell (Stanford University)[34]. For additional primary antibodies, western blot samples were transferred onto PVDF membrane (Bio-Rad) in 20 mM Tris-Base, 200 mM glycine. Alexa fluorophore conjugated anti-rabbit or anti-mouse secondary antibodies (Molecular Probes) were used according to manufacturer's specification. Fluorescence was detected on a Typhoon 9400 Variable Mode Imager (Amersham Biosciences) and quantified using ImageJ (http://rsb.info.nih.gov/ij/). Actin antibodies were provided by J. Theriot (Stanford University) and anti-cyclin B was purchased from Santa Cruz Biotechnology.

***In vitro* binding of centromere proteins to chromatin arrays.** Human and *Xenopus* CENP-C were *in vitro* translated (IVT) in rabbit reticulocyte extracts in the presence of 10 mCi ml^{-1} [^{35}S]methionine (Perkin Elmer) using the TnT Quick-Coupled Transcription/Translation system (Promega) according to the manufacturer's instructions. For a binding reaction (60 μl total volume), 5 μl of each IVT protein were mixed with chromatin arrays in bead buffer (75 mM Tris-HCl pH 7.5, 50 mM NaCl, 0.25 mM EDTA, 0.05% Triton-X-100). The final nucleosome concentration per reaction was 60 nM. Reactions were incubated at

4 °C for 1 h. The beads were washed three times with bead buffer and resuspended in 4× SDS loading buffer. Samples were separated on a SDS–PAGE, Coomassie stained and after drying scanned using a phosphorimager (Typhoon 4200, Amersham Biosciences) and quantified using ImageJ (http://rsb.info.nih.gov/ij/).

Statistical analysis. In each experiment, the relative levels of proteins associated with the chromatin arrays were normalized to values for wild type CENP-A arrays set to 1. For calculation of *P* values each data set was anchored at 1 and then log transformed followed by calculation of *P* values using a Student's *t*-test[37].

31. Luger, K., Rechsteiner, T. & Richmond, T. Preparation of nucleosome core particle from recombinant histones. *Methods Enzymol.* **304,** 3–19 (1999).
32. Lowary, P. T. & Widom, J. New DNA sequence rules for high affinity binding to histone octamer and sequence-directed nucleosome positioning. *J. Mol. Biol.* **276,** 19–42 (1998).
33. Murray, A. W. Cell cycle extracts. *Methods Cell Biol.* **36,** 581–605 (1991).
34. Kim, S., Song, E., Lee, K. & Ferrell, J. Jr. Multisite M-phase phosphorylation of *Xenopus* Wee1A. *Mol. Cell. Biol.* **25,** 10580–10590 (2005).
35. Hannak, E. & Heald, R. Investigating mitotic spindle assembly and function *in vitro* using *Xenopus laevis* egg extracts. *Nature Protocols* **1,** 2305–2314 (2006).
36. Field, C. M., Oegema, K., Zheng, Y., Mitchison, T. J. & Walczak, C. E. Purification of cytoskeletal proteins using peptide antibodies. *Methods Enzymol.* **298,** 525–541 (1998).
37. Osborne, J. W. *Best Practices in Quantitative Methods* (Sage Publications, 2008).